9 MJ RANGE GUN COMPULSATOR STATOR DESIGN AND FABRICATION

Prepared by

J. D. Herbst, K. G. Cook, R. A. Kuenast, S. B. Pratap,
R. C. Thompson, and H. D. Yun

Presented at
The 6th Electromagnetic Launch Symposium
The Institute for Advanced Technology
Austin, Texas

April 28-30, 1992

Publication No. PR-166

Center for Electromechanics
The University of Texas at Austin
Balcones Research Center
Bldg. 133, EME 1.100
Austin, TX 78758-4497
(512) 471-4496

9 MJ Range Gun Compulsator Stator Design and Fabrication

J. D. Herbst, K. G. Cook, R. A. Kuenast, S. B. Pratap, R. C. Thompson, and H. D. Yun
Center for Electromechanics
The University of Texas at Austin
Austin, TX 78712

Abstract--The range gun compulsator is a self excited, air-cored alternator designed to provide pulsed power in a field portable electromagnetic launch system capable of accelerating a salvo of nine projectiles to a muzzle energy of 9 MJ at velocities ranging from 2.5 to 4.0 km/s [1]. The compulsator is designed to deliver 3.2 MA current pulses to a railgun launcher at a peak power rating of 10 GW. The stator consists of a multi-turn compensating winding with a laminated stainless steel support structure, an aluminum excitation field coil and support structure, a stainless steel stator casing and main end plates, hydrostatic bearings, seals, support pedestals, and current collection mechanisms for the field excitation and main armature circuits.

The two-pole compensating winding provides selective passive compensation for the main armature, generating a flat-topped current waveform and limiting projectile acceleration. The room temperature field coil operates at 41.5 kA peak current and generates an average 2.1 Tesla radial field at the rotor perimeter. The stator casing and end plates are stainless steel weldments, with a ribbed design to reduce weight without sacrificing stiffness. The rotor is supported on hydrostatic fluid film bearings with high performance segmented carbon ring seals. There are two discrete current collection systems; the field excitation system operates at 17 kV and 41.5 kA, and the armature system operates at 6 kV and 3.2 MA. Several novel techniques were used to improve the high voltage electrical insulation in the brush mechanisms and manage the large magnetic forces generated during discharge.

Electromagnetic finite element techniques were used to calculate the magnetic field distribution and induced currents in the stator structure. The results of this analysis were used to calculate loading distributions on the stator structures, which were applied to detailed finite element models for stress and deflection analyses of the stator components.

This paper will provide a brief summary of the structural analysis of the compulsator stator as well as a detailed description of the major stator components. Fabrication and assembly techniques will also be presented, along with the current status of the project.

Electromagnetic And Structural Analysis

Electromagnetic analysis of the compulsator stator was performed using a three-dimensional (3-D), transient electromagnetic finite element code developed at CEM-UT. A dynamic circuit simulation was used to generate current distribution in the windings as a function of rotor position. These current distributions were then input into the electromagnetic analysis code, which provides calculated eddy current, flux density, and J x B force distributions for the stator components. Electromagnetic analysis results were used as inputs to a 3-D finite element structural analysis model run using ABAQUS®. PATRAN® software was used during pre- and post-processing for finite element mesh generation and visualization of analysis results. Analyses were performed at both minimum and maximum inductance positions, which represent the extremes of armature flux distribution and loading variations. At minimum inductance position, flux is confined to the region between the armature and compensating windings, with the majority of the load appearing on the compensating winding. At maximum inductance position, armature flux penetrates the compensating winding, generating eddy currents in the conductive portions of the stator structure. This configuration results in an extremely complex force distribution and represents the most severe loading on the stator components.

The work was supported by U.S. Army ARDEC, contract no. DAAA21-86-C-0281.

Stator Mechanical Design

The stator structure provides mechanical support for the compulsator rotor bearings, compensating winding, and excitation field coil, and provides the compliant reaction path to ground for the discharge forces. A compulsator cross section identifying some of the major stator components is shown in fig. 1.

Laminated Support Structure

The compensating winding support structure is laminated to minimize eddy current losses and is fabricated of 1.21 mm thick, half-hard 301 stainless steel sheet adhesively bonded with 0.2 mm thick glass reinforced epoxy. The half-hard 301 stainless steel material was selected based on a combination of high mechanical properties with limited magnetic permeability and low saturation flux density.

The laminated structure is made up of two basic shapes, seven annular sections with three segments per layer separated by six extended support plates with two segments per layer. The lamination layers were built of multiple segments to allow use of work hardened 301 stainless steel material and minimize the scrap associated with the stamping of the part profiles. The part profiles include features to provide maximum bond area and support for the compensating winding conductors, and connection points for

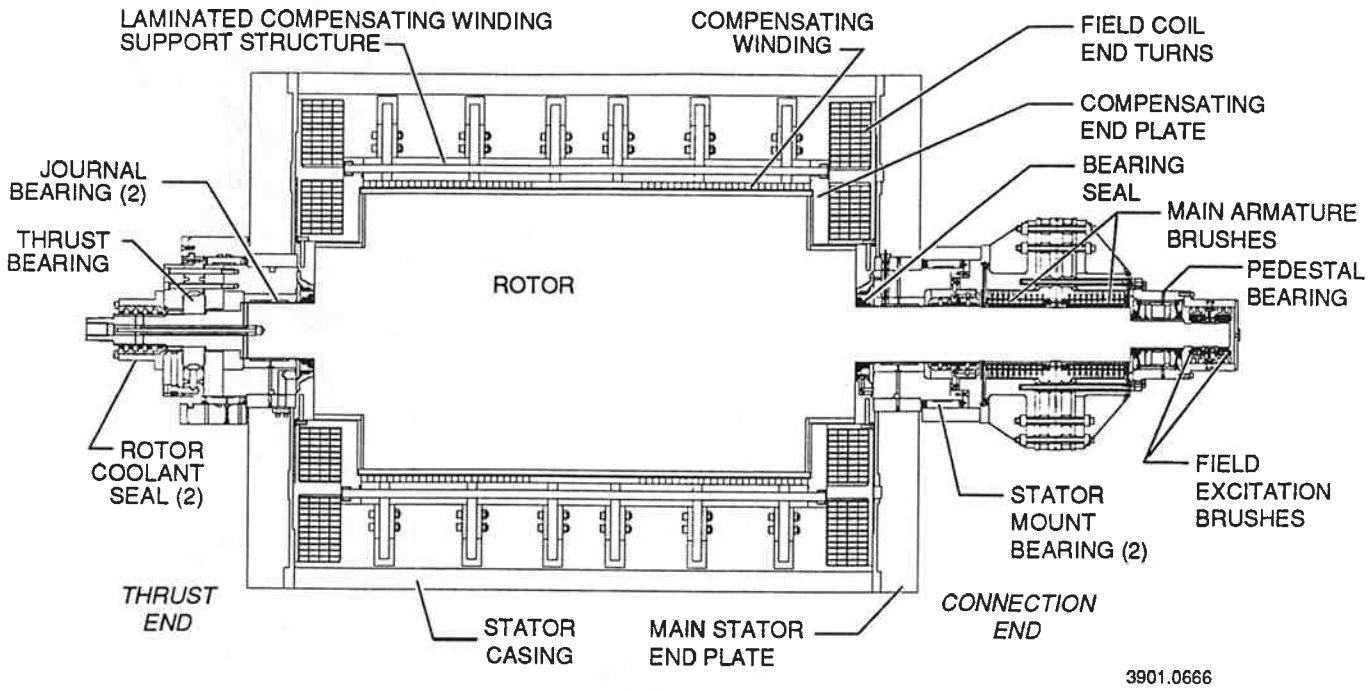

Fig. 1. Compulsator cross section

other stator components. To prepare the surface for adhesive bonding, the bond surfaces were solvent washed, acid etched to remove oxides, and then coated with an epoxy primer. The preimpregnated fiberglass adhesive was cut to match the segment profile and 5 cm thick subsections were assembled, aligned with dowel pins, and cured. Finally, the subsections were assembled and bonded to form the complete structure, shown in fig. 2.

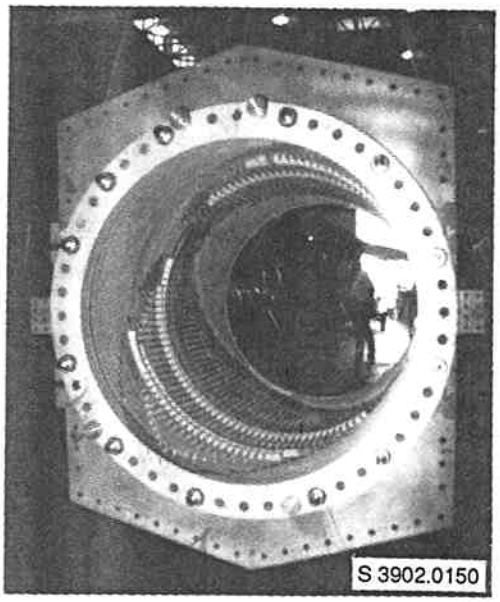

Fig. 2. Photo of assembled laminated compensating winding support structure

Compensating Winding

The two-pole compensating winding provides selective passive compensation for the main armature, generating a flat-topped current waveform and limiting projectile acceleration [2]. The compensating winding consists of 26 shorted turns per pole, and is epoxy potted into support slots in the laminated support structure. Each conductor is fabricated of aluminum litz wire compacted into a nominal 2.5 cm square cross section, with additional insulation and support for the conductor provided by a glass fiber overbraid. To form the shorting connections in the compensating winding conductors, the polyamide-imide insulation is stripped from the litz wire strands using a high temperature alkali salt bath. After the exposed aluminum has been acid etched to remove surface contamination and oxides, the wires are tinned with a 91% tin, 9% zinc solder. The ends of the conductor are compacted and inserted into a copper crimp lug, which is then radially compressed to complete the connection.

Compensating End Plates

Axial electromagnetic and field coil support loads on the stator are primarily reacted through an array of forty-eight, 17-4PH stainless steel axial tie bars running through the compensating winding support structure. The axial tie bars connect the two 17-4PH compensating end plates and provide an initial axial compressive preload on the compensating winding support structure. The 17-4PH stainless steel was selected for a combination of high mechanical properties with relatively low magnetic permeability and saturation flux density. To prevent galling of threads on the tie bars, beryllium copper was selected for

the nut material. The tie bars are insulated from the compensating end plates and laminated support structure to prevent global circulating currents.

A support beam extends axially from the outboard face of the compensating end plate to provide structural support for the attractive and axial loads generated by the field coil. The lateral profiles of the end turn support beam match the formed profile of the field coil conductors, transferring the attraction loads between coil halves around the rotor flywheel extension. Bolted joints through the field coil central support plates transfer field coil axial loads through the compensating end plate to the axial tie bars. Additional field coil axial loads are reacted to the axial tie bars through the field coil outer support structure and the outboard face of the end turn support beam.

Secondary Eddy Current Shields

Conductive eddy current shields have been placed between the compensating winding and field coil to reduce coupling between the field coil and rotor armature conductors at maximum inductance position. The upper secondary shields are machined of 7075-T751 aluminum and the lower secondary shields are machined of 6061-T6 aluminum. Electromagnetic forces on the secondary shields are reacted to the laminated compensating winding support structure through bolted connections. The upper secondary shields also provide axial support for the laminated support plates and additional lateral support for the field coil central support plates. At the compulsator's maximum inductance position, the rotor armature and primary compensating windings are 90^0 out of phase and there is no coupling between the two windings. Without secondary shielding, flux from the armature currents would penetrate past the compensating winding and couple with the field coil, creating a transient current spike and greatly increasing magnetic loading on the coil. Image currents in the secondary eddy current shields partially compensate the armature discharge currents, shielding the field coil, while still providing the increase in inductance necessary for current profile shaping [2].

Excitation Field Coil

The compulsator field coil consists of two discrete halves connected to form a solenoidal series winding. This provides a uniform distribution of radial flux over the voltage generating region of the armature winding and reduces the shear stresses on the armature winding conductors [3]. The field coil stores approximately 40 MJ at a peak current of 41.5 kA, and provides an average 2.1 Tesla radial field density at the rotor perimeter. To minimize charging time and the associated resistive and armature reaction losses, the field coil is driven by a 17 kV, Silicon Controlled Rectifier (SCR), rectified excitation armature built into the rotor structure [3], [4]. Each coil half is made up of 20 individual four turn layers of 1.9 cm thick 1100-H14 aluminum plate, with a total of 75 effective turns per half. The individual plates were spirally cut, formed, sleeved with fiberglass cloth, assembled, and then welded together. Each coil half includes a 5 cm thick, 2219-T87 aluminum internal support plate and is housed in an external support structure comprised of 1.6 cm thick, 2219-T87 aluminum plates. The exposed conductor surfaces are covered with a preimpregnated fiberglass cloth, and the structure is vacuum impregnated to provide electrical insulation and structural integrity.

Loads on the field coil conductors are generated due to internal magnetic forces, as well as interaction of the field coil conductor currents with the armature discharge flux. To minimize mechanical stresses in the conductors, these loads are reacted through connections between the field coil support structure and the laminated compensating winding support structure, main stator end plates, end turn support beam, and stator casing. Along the active length of the field coil, keys machined into the inner edge of the 5 cm thick central support plate engage with mating keys stamped into the outer profile of the annular compensating winding support structure laminations. The upper and lower edges of the field coil outer support housing extend beyond the conductors and are bolted to connection bars attached to the laminated compensating winding support plates. The end turns of the field coil are supported through bolted connections to the compensating end plates and field coil end turn support beam assembly. An additional compression support, at the upper edge of the end turn support housing, transfers field coil loads directly to the main stator end plates. Fig. 3 is a photo of the assembled left field coil half and support structure.

The conductor profile and plate interconnection features were generated using a two axis Ingersoll Rand NC abrasive waterjet cutting system. After cutting, the end turn sections of the conductor plates were formed to provide clearance for flywheel extensions. The conductor edges were radiused to reduce voltage concentrations, and the surfaces were grit blasted to remove contamination and improve adhesion. The conductor plates were then acid-etched to thoroughly clean and de-oxidize the surface, and an epoxy primer was applied and cured.

Prior to assembly of the conductor plates, a 0.45 mm thick braided E-glass sleeve with an epoxy compatible sizing was applied to each conductor. To minimize areas of unsupported epoxy and improve electrical insulation between the conductors, additional layers of E-glass cloth and 0.28 mm thick dacron/mylar/dacron (DMD) sandwich insulation were installed during coil assembly.

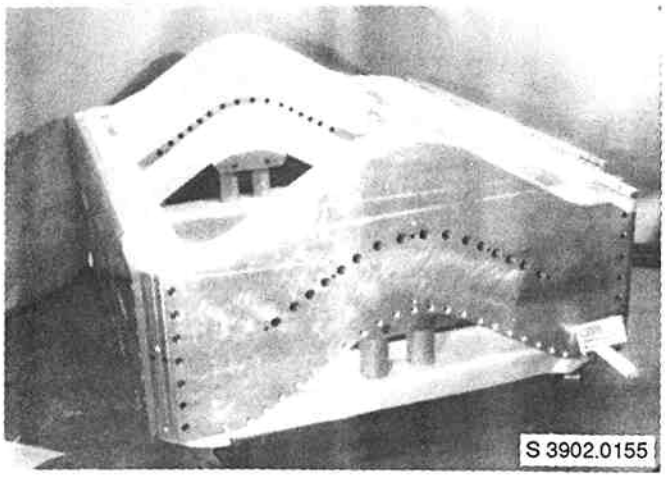

Fig. 3. Photo of assembled field coil with support structure

To eliminate inaccessible mechanical connections, welded joints were used to connect the individual conductor plates in the assembly. Tabs welded into the lower conductor plate fit into mating slots in the upper plate generated during the waterjet cutting process. The tabs were then TIG welded to the upper conductor, creating an extremely low resistance electrical connection between plates. Heating of areas adjacent to the welds was controlled through the use of water cooled copper heat sinks to prevent degradation of the epoxy primer and charring of the fiberglass sleeving. Customized plugs were installed through insulated penetrations in the central support plate to continue the series electrical connection of the coil. When all 20 plates were assembled, the outer support housing was installed and bolted to the central support plate. The central support plate and outer support housing are circumferentially discontinuous to minimize coupling with the field coil, with layers of preimpregnated cloth and DMD used to provide electrical insulation.

A thin layer of cured epoxy prepreg is used to complete the containment of the conductors and central support plate assembly, and a vacuum pressure impregnation process is used to transfer resin to the evacuated mold. The vacuum impregnation procedure minimizes void content and allows additional resin to be transferred to the mold to compensate for shrinkage during the cure cycle. A DOW D.E.R. 332 epoxy resin system with additives to reduce viscosity and improve cured ductility was used in this application.

Main Stator End Plates and Casing

Support and location for the compulsator rotor relative to the compensating winding and field coil is provided through hydrostatic bearings supported by the central hub of the main stator end plate. Axial extensions of the radial bearing housings provide the primary mounting surfaces for the compulsator mount bearings and pedestals. The stator casing separates the two main end plates and provides the structural connection between the compensating winding support structure and the main end plates. The stator casing also provides structural connections for the stator compliant mount dampers. The stator end plates and casing are fabricated 304 stainless steel structures, with a ribbed design to provide required stiffness with minimum weight.

Rotor Hydrostatic Bearing System

Axial and lateral support of the 10,000 lb compulsator rotor is derived from hydrostatic fluid film radial and thrust bearings. Hydrostatic bearings were selected for their high stiffness and damping characteristics, and because these parameters can be easily adjusted as required during initial testing. The bearing sumps are isolated with circumferential segmented carbon ring seals and are actively scavenged. Fig. 4 shows the compulsator bearing insert and seal assemblies.

CEM-UT has developed sophisticated computer codes for analyzing high performance hydrostatic bearing systems [4]. These codes include a two-dimensional (2-D) formulation of the Reynolds' equation for laminar flow, with the unique capability to evaluate the effects of shaft tilt and bearing deformation on bearing performance. Data output from the program includes direct and cross coupled stiffness and damping coefficients, flow rate, power losses for the bearing lands and recesses, oil temperature rise, load capacity, attitude angle, and pressure distributions as a function of increasing eccentricity ratio and shaft tilt. During initial testing, real time data monitoring will provide a means for evaluating bearing performance.

Radial Hydrostatic Bearings

The main radial hydrostatic bearing inserts are machined from aluminum bronze with 1.59 cm wide lands and bored for a 22.098 cm diameter shaft. The bearing inserts are interference fit into heavy stainless steel bearing housings which are in turn supported by the central hub of the main stator end plate. Each main radial bearing is supplied with 3,000 psi oil at 40 gpm.

Bearing clearance varies with shaft speed due to thermal changes in both the bearings and stator structure as well as thermal and spin effects of the shaft. Calculated temperatures were applied to a finite element model of the stator structure to generate thermal growth data. This data was then used to determine the required initial bearing clearance. Increased bearing stiffness due to a reduction in radial clearance is offset by a reduction in oil viscosity due to higher temperatures from increased frictional heating. These two effects tend to maintain a uniform bearing stiffness over the operating speed range, which minimizes dynamic shaft displacements during critical speed excursions. Bearing stiffness increases dramatically during the discharge cycles due to eddy current heating of the shaft and the associated thermal growth which further reduces the radial clearance of the bearing.

Hydrostatic Thrust Bearing

The rotor thrust bearing is a five pocket, opposed pad hydrostatic bearing, with an axial stiffness of 30.0E6 lb/in. The thrust bearing has an initial clearance of 0.005 in., and is supplied with 3,000 psi oil at a flow rate of 55 gpm. The thrust bearing assembly consists of two 7.62 cm thick, 17-4 PH stainless steel bearing plates separated by an annular 17-4 PH spacer. The thrust runner is fabricated of 17-4 PH stainless steel with a Nedox coating.

Hydrostatic Brush Bearing

To prevent excessive whirl of the small diameter connection end shaft, a hydrostatic bearing has been incorporated between the armature and field excitation brush

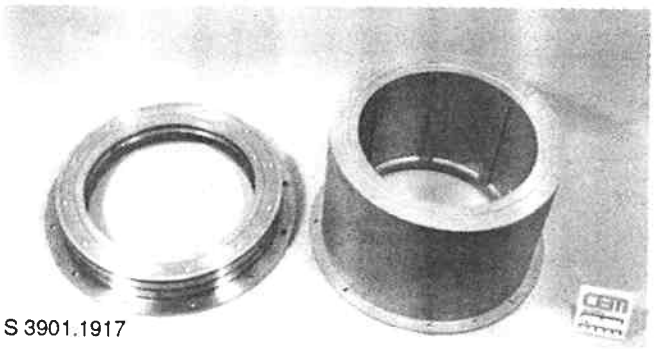

Fig. 4 Photo of radial hydrostatic bearing inserts and seal assemblies

mechanisms. Shaft whirl contributes to jitter in the brushes, which can create arcing between the brush and slip ring. The brush bearing is a four pocket, 12.065 cm diameter hydrostatic bearing with a flow rate of 15 gpm. Due to varied operating parameters, bearing stiffness ranges from 2.0 to 5.0 x 10^6 lb/in. and damping from 1.0 to 3.0 x 10^3 lb-s/in. The brush bearing housing is directly connected to ground through an independent mount pedestal.

Shaft Seals

The compulsator hydrostatic bearing and rotor coolant systems incorporate six separate circumferential shaft seal assemblies. The seals are gas buffered, segmented carbon rings with interface velocities up to 350 ft./s. At high speeds, surf-boarding instabilities are minimized by negative-lift pockets machined in the carbon segments.

Inboard radial bearing seals isolate bearing lubricant in the inboard radial bearing sumps from the evacuated rotor cavity. The non-thrust end outboard radial bearing seal is incorporated into the rotor coolant seal assembly, which provides isolated flow paths for ethylene-glycol/water coolant for the rotor eddy current shields. The outboard thrust bearing seal has also been incorporated into the thrust end rotor coolant seal assembly. The outboard radial bearing and inboard thrust bearing share a common sump cavity. An additional set of seals is used to isolate the brush bearing sumps from the brush mechanisms.

Stator Support Structure

The compulsator is supported on two radial hydrostatic bearings which are mounted in stainless steel support pedestals. Design for the pedestals included requirements for appropriate structural characteristics to optimize compulsator dynamics. To reduce the magnitude of the discharge torque transmitted to the compulsator mount structure, the compulsator stator structure is allowed to compliantly rotate approximately 10 degrees against a set of 12 hydraulic dampers.

Compulsator Mount Bearings

During compliant rotation, the compulsator stator is supported on two radial hydrostatic bearings. Hydrostatic bearings were selected for their unique damping characteristics and will operate in combination with the rotor bearings to reduce rotor imbalance forces. CEM-UT rotor dynamic codes were again used to design the compulsator mount bearings.

The mount bearing inserts are machined from aluminum bronze centrifugal castings, and the bearing housings are fabricated of 17-4 PH stainless steel. The bearings fit over machined extensions of the rotor radial bearing housings and provide support for the entire weight of the compulsator. Elastomeric seals isolate the mount bearing sumps from atmospheric pressure.

Stator Support Pedestals

The compulsator mount bearings are connected to ground through two stator support pedestals. The pedestals are fabricated and welded 17-4PH stainless steel structures designed to minimize deformation of the mount bearings, and provide vertical and lateral support for the compulsator. A finite element analysis of the pedestal structure was performed to calculate structural deformations and induced stresses due to static loading.

A parametric study involving the pedestal structure and pedestal bearing was also performed. The study focused on compulsator dynamic response during critical speed excursions as the pedestal and pedestal bearing stiffness and damping were varied. Using CEM-UT rotor dynamics code with a frequency response analysis, compulsator dynamic response was determined for combinations of the above parametric values. The studies did not identify strong sensitivities between pedestal structure or pedestal bearing properties and compulsator dynamic response, except for the large dynamic response when pedestal bearing damping approached zero. This sensitivity to the lack of pedestal bearing damping is the basis for using hydrostatic bearings instead of rolling element bearings. Dynamic displacement and force reductions through the inclusion of pedestal bearing damping will allow the compulsator to operate with a larger margin of safety at the design allowable rotor imbalance.

Compliant Mount Dampers

A series of 12 compliant mount dampers absorb the energy of the rotation of the stator during discharge and transmit the discharge torque to ground. The mount dampers are connected to the stator structure at the apex rib of the main stator casing, with six tension and six compression units. The damper loading is defined by the torque/time history of the field excitation and discharge sequence, and the design was constrained by the maximum allowable transmitted load and stator rotation. The selected dampers are a modified crane buffer with damping and spring coefficients optimized to allow operation over a wide range of energy levels.

Brush Mechanisms

The 9 MJ compulsator includes two discrete current collection mechanisms, one for connection of the excitation armature to the field current rectification system and one to connect the primary armature winding to the gun switch modules. Each brush mechanism presents unique design challenges. The excitation brush mechanism operates at 17 kV and 41.5 kA, with high voltage electrical insulation and large integrated I^2t values being the primary concerns, while the armature brush mechanism operates at 6 kV and 3.2 MA, with internal magnetic forces, current distribution and ohmic heating presenting the greatest design difficulties. Where possible, existing proven design features were incorporated into both brush mechanisms. Fig. 5 is a detail of the armature brush/strap assembly; the excitation brushes assembly is similar, but does not include the series resistors or conductive flux reduction plates.

Field Excitation Brush Mechanism

Each terminal of the excitation brush mechanism is made up of eight circumferential rows of three brushes. The brushes operate at a nominal current density of 0.585 kA/cm^2. The brushes are formed by silver brazing a 0.635

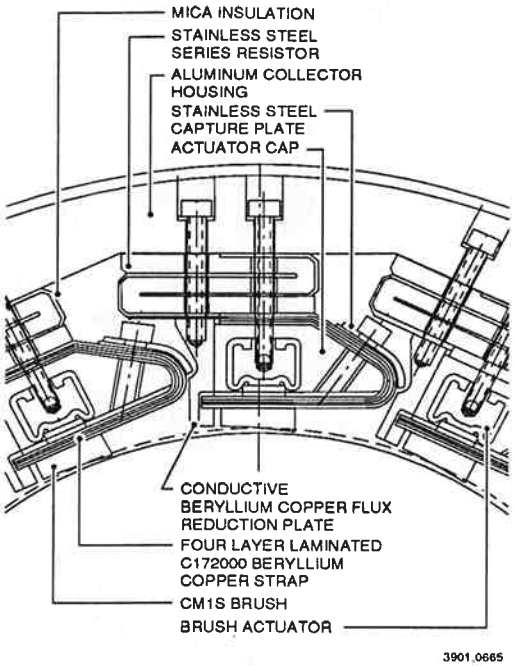

Fig. 5 Armature brush mechanism cross section

cm x 1.27 cm x 1.91 cm block of Morganite CM1S copper graphite to three laminated strips of Glidcop AL-15 dispersion strengthened copper. The straps are reinforced with an insulated stainless steel capture plate bolted to the actuator cap with insulated stainless steel screws. Brush actuation and contact force is provided by an actuator comprised of a Viton bladder molded over a cast aluminum bronze core, with 150 psi actuation pressure supplied by bleed air from the prime power gas turbine. Bleed air is also used to provide buffer flow to the center of the labyrinth seal between the two terminals of the brush mechanism, limiting the entrance of brush debris into this region and preventing build up of surface conductivity with the associated tracking breakdown of the insulation system. Current from the brush assemblies is transferred to an aluminum collector ring mounted in a G-10 composite support housing. Flexible cables are used to connect the current collector rings to the SCR rectification system.

In order to verify the integrity of the high voltage insulation system operating in an enclosed environment that includes conductive brush debris, a full scale mock-up of the excitation brush mechanism was fabricated and tested at speeds up to 8,500 rpm and voltages of 25 kV with no insulation failures. Thermal imaging techniques were also used to gather data on the temperature distribution in the excitation brush mechanism during the relatively long field coil excitation sequence.

Armature Brush Mechanism

Much of the fabrication and high voltage insulation techniques developed for the excitation brush mechanism were incorporated into the design of the armature brush mechanism, but current distribution and electromagnetic loading issues unique to extremely high current systems also had to be addressed. Each terminal of the armature brush mechanism is made up of 14 circumferential rows of 16 brushes, operating at a nominal current density of 5.90 kA/cm^2. The CM1S brushes are silver brazed to a four layer, laminated C17200 beryllium copper strap assembly.

Rotor shaft diameter and brush current density constraints dictated the use of small diameter, axially long brush slip rings. While this configuration limits the slip speed of the brush/ring interface, it creates transient current distribution problems due to inductively preferential current paths through the inner rows of brushes in each terminal. The final design includes the separation and electrical isolation of individual brush pairs between the slip ring and the current collector housing along with the incorporation of additional resistance into each current path. The four layer laminated strap assemblies are terminated into a stainless steel series resistor to provide the additional resistance. Electromagnetic analysis and laboratory testing were used to evaluate the final design.

In addition to internal compensation and terminal interaction forces, magnetic coupling between the brush strap currents and uncompensated currents in the rotor shaft conductors generate large axial forces on the brushes. Along with the stronger four layer laminated strap assembly, conductive beryllium copper flux reduction plates have been included between each circumferential row of brushes. During the initial current rise at the beginning of the discharge pulse, when nonuniform current distribution is most prevalent, eddy currents in the flux reduction plates shield the brushes from circumferential magnetic fields. As the current pulse progresses, the eddy currents and nonuniformity of the transient current distribution diminish together. To further strengthen the brushes, an insulated tab extending from the strap assembly engages a slot in the flux reduction plates, allowing radial actuation travel, but preventing axial motion of the brush.

Current Project Status

At this time, the major compulsator stator components are in the final phases of fabrication and assembly. The compensating winding support structure has been completed along with final assembly of the field coils. The stator casing and compensating end plates are in final machining, and the brush mechanisms are essentially complete. Initial assembly of the stator structure for line boring should begin during January 1992. Laboratory testing of the compulsator power supply should begin in April 1992.

REFERENCES

[1] W. A. Walls, et al., "A Field Based, Self Excited Compulsator Power Supply for a 9 MJ Railgun Demonstrator," *IEEE Transactions on Magnetics*, Vol. 27, No. 1, January 1991, pp 335-340..

[2] M. D. Driga, S. B. Pratap, and W. F. Weldon, " Design of Compensated Pulsed Alternators with Current Waveform Flexibility," Digest of Technical Papers, 6th IEEE Pulsed Power Conference, Arlington, VA, 1987, pp 111-114.

[3] S. B. Pratap, K. T. Hsieh, M. D. Driga, and W. F. Weldon, "Advanced Compulsators for Railguns," *IEEE Transactions on Magnetics*, Vol. 25, No. 1, January 1989, pp 454-459.

[4] R. N. Headifen, "Rotordynamic Modeling of Flexible Rotor Machines Supported with Hydrostatic Bearings," Ph.D. Dissertation, The University of Texas at Austin, December 1991, unpublished.